Diminished Induction of Skin Fibrosis in Mice with MCP-1 Deficiency

Ahalia M. Ferreira[1], Shinsuke Takagawa[2], Raoul Fresco[3], Xiaofeng Zhu[4], John Varga[2] and Luisa A. DiPietro[1]

Scar and fibrosis are often the end result of mechanical injury and inflammatory diseases. One chemokine that is repeatedly linked to fibrotic responses is monocyte chemoattractant protein-1 (MCP-1). We utilized a murine fibrosis model that produces dermal lesions similar to scleroderma to evaluate collagen fibrillogenesis in the absence of MCP-1. Dermal fibrosis was induced by subcutaneous injection of bleomycin into the dorsal skin of MCP-1−/− and wild-type C57BL/6 mice. After 4 weeks of daily injections, bleomycin treatment led to thickened collagen bundles with robust inflammation in the lesional dermis of wild-type mice. In contrast, the lesional skin of MCP-1−/− mice exhibited a dermal architecture similar to phosphate-buffered saline (PBS)-injected control and normal skin, with few inflammatory cells. Ultrastructural analysis of the lesional dermis from bleomycin-injected wild-type mice revealed markedly abnormal arrangement of collagen fibrils, with normal large diameter collagen fibrils replaced by small collagen fibrils of 41.5 nm. In comparison, the dermis of bleomycin-injected MCP-1−/− mice displayed a uniform pattern of fibril diameters that was similar to normal skin (average diameter 76.7 nm). The findings implicate MCP-1 as a key determinant in the development of skin fibrosis induced by bleomycin, and suggest that MCP-1 may influence collagen fiber formation *in vivo*.

Journal of Investigative Dermatology (2006) **126,** 1900–1908. doi:10.1038/sj.jid.5700302; published online 11 May 2006

INTRODUCTION

When tissue is damaged, whether by mechanical trauma or inflammation, the repair process is initiated. Under ideal circumstances, inflammation quickly resolves, and tissue repair occurs in a regulated fashion. However, in many disease states, and sometimes even following minimal traumatic insult, tissue repair becomes severely dysregulated, and undue fibrosis results. Pathologic fibrosis is characterized by excessive accumulation of extracellular matrix (ECM) proteins (Knapp *et al.*, 1977; Hunt, 1990). In normal physiological tissue remodeling, a careful balance between collagen synthesis and degradation is maintained, culminating in a final collagen content that is similar, although not identical, to the original tissue (Parks, 1999). The matrix metalloproteinases (MMPs) and their inhibitors (tissue inhibitor of metalloproteinases (TIMPs)) play a crucial role in the maintenance of the normal balance between ECM synthesis and degradation (Matrisian, 1992; Parks, 1999). During fibrosis, the equilibrium shifts, and decreased levels of MMPs and increased levels of TIMPs are thought to create an environment that favors ECM accumulation.

In addition to the MMPs and their inhibitors, several other proteins have been shown to modify collagen formation and to influence the fibrotic response. Heat-shock protein 47 (HSP47), a collagen-specific intracellular chaperone, is essential during the early stages of collagen biosynthesis. Overexpression of HSP47 promotes collagen accumulation, contributing considerably to the development of fibrotic conditions (Masuda *et al.*, 1994; Razzaque *et al.*, 1998; Dafforn *et al.*, 2001).

In tandem with the net increase in collagen synthesis and accumulation that occurs in fibrotic tissues, an altered collagen ultrastructure is also apparent. Collagen fibrils in fibrotic tissue are often smaller and less uniform in size than fibrils in normal tissue (Fleischmajer *et al.*, 1978; Lakos *et al.*, 2004). The assembly of collagen into fibrils is regulated by a number of factors, including the small leucine-rich proteoglycans (Iozzo, 1997; Soo *et al.*, 2000). Within this proteoglycan family, several members, including decorin, fibromodulin, and lumican, have a key function in collagen assembly. Decorin, fibromodulin, and to a lesser degree, lumican, bind to fibrillar collagen and influence fibril diameter, tissue architecture, and strength (Soo *et al.*, 2000).

Many studies suggest that the dysregulated collagen synthesis that typifies a fibrotic response is initiated by soluble mediators generated during uncontrolled inflammation.

[1]*Department of Surgery, The Burn and Shock Trauma Institute, Loyola University Medical Center, Maywood, Illinois, USA;* [2]*Section of Rheumatology, Feinberg School of Medicine, Northwestern University, Chicago, Illinois, USA;* [3]*Department of Pathology, The Burn and Shock Trauma Institute, Loyola University Medical Center, Maywood, Illinois, USA and* [4]*Department of Preventive Medicine and Epidemiology, Loyola University Medical Center, Maywood, Illinois, USA*

Current address and Correspondence: Dr Luisa A. DiPietro, Department of Periodontics (MC 859), UIC - College of Dentistry, 801 S. Paulina Street, Chicago, IL 60612-7211. E-mail: ldipiet@uic.edu

Abbreviations: ECM, extracellular matrix; GAPDH, glyceraldhehyde-3-phosphate-dehydrogenase; HSP47, heat-shock protein 47; MCP-1, monocyte chemoattractant protein-1; MMP, matrix metalloproteinase; PBS, phosphate-buffered saline; α-SMA, alpha-smooth muscle actin; TGF-β, transforming growth factor-beta; TIMP, tissue inhibitor of metalloproteinase; WT, wild-type

Received 1 June 2005; revised 31 October 2005; accepted 31 January 2006; published online 11 May 2006

Monocyte chemoattractant protein-1 (MCP-1), a multifunctional inflammatory chemokine belonging to the C–C chemokine superfamily, has been shown to be upregulated in a variety of fibrotic conditions. These include idiopathic pulmonary fibrosis, systemic sclerosis, and bleomycin-induced murine scleroderma (Rollins, 1996; Lloyd *et al.*, 1997; Hasegawa *et al.*, 1999; Distler *et al.*, 2001; Yamamoto and Nishioka, 2003). The involvement of MCP-1 in these pathological states has generally been thought to reflect its pro-inflammatory role, as the generation of the inflammatory milieu influences fibroblast function and collagen synthesis. However, recent evidence suggests a more direct effect of MCP-1 as well, as MCP-1 has now been shown to directly upregulate type I collagen gene expression in rat lung fibroblasts *in vitro* by modulating transforming growth factor-beta (TGF-β) expression in fibroblasts themselves (Gharaee-Kermani *et al.*, 1996). In addition, MCP-1 also induces increased levels of MMP-1 and -2, as well as TIMP-1, in cultured skin fibroblasts. When taken together, these observations indicate that in fibrotic diseases, the function of MCP-1 may extend well beyond its role as a pro-inflammatory mediator, and may include direct modulation of ECM synthesis by the fibroblast.

The current study was performed in order to assess the potential roles of MCP-1 in development of pathological fibrosis. A well-established *in vivo* model of skin fibrosis was used to evaluate both inflammation and collagen ultrastructure in the presence and absence of MCP-1. In this murine model, subcutaneous injection of bleomycin produces a dermal lesion that is histologically and biochemically similar to that seen in scleroderma (Yamamoto *et al.*, 1999). The results presented here suggest that MCP-1 influences both inflammation and collagen ultrastructure in this model.

RESULTS

Histologic comparison of bleomycin-induced lesions in wild-type and MCP-1−/− mice

The accumulation and organization of dermal collagen, and the degree of fibrosis were compared between wild-type and MCP-1−/− mice that had received daily injections of bleomycin for 4 weeks. Sections were subjected to Masson's trichrome stain, which permits areas of mature collagen deposition to be detected. Skin lesions from bleomycin-treated wild-type mice showed dense accumulation of thick collagen bundles in the dermis, reflecting increased collagen deposition. There was replacement of subcutaneous fat by connective tissue (Figure 1a). Lesional dermis contained a marked mononuclear cell infiltration, predominantly localized to the deeper layer (Figure 1a). In contrast, bleomycin injection sites from MCP-1−/− mice developed significantly less dermal fibrosis and the subcutaneous fat was partially preserved (Figure 1a). Mononuclear infiltration was also reduced in skin lesions from MCP-1−/− mice.

To provide a quantitative assessment of fibrosis, dermal thickness was measured. In wild-type mice, the dermal thickness of bleomycin lesions was increased 2-fold over control phosphate-buffered saline (PBS)-injected sites (369.5 *vs* 150.3 μm, $P<0.0001$). In contrast, in MCP-1−/− mice, bleomycin induced only a modest increase in dermal thickness (Figure 1b). Interestingly, both PBS-injected (Figure 1b) and untreated skin (data not shown) of MCP-1−/− mice exhibited dermal thickness that was greater than in wild-type mice. However, in contrast to wild-type mice, bleomycin injection of MCP-1−/− mice resulted in only a minimal (1.2-fold) increase in dermal thickness compared with PBS-treated controls (261.8 *vs* 196 μm, $P=0.092$) (Figure 1b). Therefore, the fibrotic response induced by bleomycin was greatly reduced in MCP-1−/− mice compared to wild-type control.

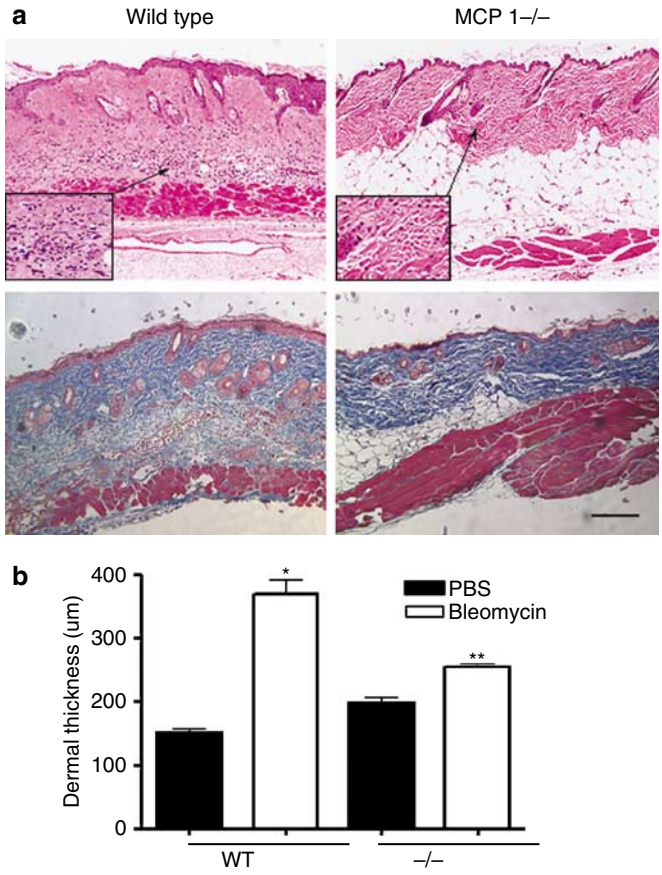

Figure 1. Histological assessment of bleomycin-induced lesions in wild-type (WT) and MCP-1−/− mice. Photomicrographs of bleomycin-injected sites from WT and MCP-1−/− mice. (**a**) WT (left panels) and MCP-1−/− (right panels) mice received daily subcutaneous injections of PBS or bleomycin for 4 weeks. Lesional skin was harvested and examined by histology. Representative sections stained with either hematoxylin and eosin (upper panel) or Masson's trichrome staining (lower panel) are shown (original magnification $\times 100$). Insets in upper panels show a higher magnification (original magnification $\times 400$), and demonstrate a higher degree of inflammatory cell infiltration in lesions from WT than MCP-1−/− mice. Bar = 100 μm. (**b**) Dermal thickness was measured at five randomly selected sites/field for PBS and bleomycin-injection sites in both WT and MCP-1 −/− mice. Results are expressed as the means ± SEM, *$P<0.0001$ versus WT PBS treatment; **$P<0.005$ against WT bleomycin treatment. WT, $n=4$, MCP-1−/− mice, $n=5$.

Collagen fibril diameter following bleomycin injection

Following 4 weeks of daily bleomycin injections, the skin from wild-type and MCP-1−/− mice ($n=4$) was examined by transmission electron microscopy for changes in the ultra-

structure of collagen fibrils. In wild-type mice, the injection of bleomycin led to a markedly abnormal arrangement of collagen fibrils. The large diameter collagen fibrils that are present in normal skin were largely replaced by small fibrils in lesional skin (Figure 2a and b). Similar reductions in fibril diameter have been described in fibrotic responses, and this change is generally representative of active fibrosis and rapid collagen synthesis (Kischer, 1974; Fleischmajer *et al.*, 1978). In contrast, skin from bleomycin-injected MCP-1−/− mice exhibited fibrils with a more uniform pattern of fibril diameter and distribution, with an average diameter comparable to that of normal skin (Figure 2). Morphometric analysis demonstrated that the average collagen fibril diameter at sites of bleomycin injection was significantly different in MCP-1−/− and wild type mice (76.7 ± 6.1 *vs* 41.5 ± 4.2 nm), $P = 0.0339$ (Figure 2b). Surprisingly, measurement of cross-sectional collagen fibrils from lesional skin from MCP-1−/− mice also revealed the presence of very large fibrils up to 227 nm with abnormal shape, suggesting lateral fusion of several adjacent fibrils. These fusions were not considered when calculating collagen fibril diameter distributions (Figure 2a, right panel, inset).

Inflammatory cell and myofibroblast content in lesional skin

To characterize the degree and type of inflammatory cell infiltration in the lesional dermis, immunohistochemical markers were used to identify and quantify neutrophils, macrophages, and T lymphocytes. When compared to wild-type mice, bleomycin-treated skin from MCP-1−/− mice exhibited significantly fewer macrophages (115 ± 1.4 *vs* 57.1 ± 3.5 per high-powered fields) (Figure 3a). Quantification of neutrophils revealed that bleomycin-induced fibrotic skin from MCP-1−/− mice also contained significantly less neutrophils than the corresponding lesion in wild-type mice (11.4 ± 1.3 *vs* 18.9 ± 1.0 per high-powered fields) (Figure 3b). In contrast to macrophages and neutrophils, the levels of CD3 positive T cells were not significantly different in bleomycin skin from wild-type and MCP-1−/− mice (Figure 3c). No differences between wild-type and MCP-1−/− mice were seen for the numbers of neutrophils, macrophages, or T cells in control sites that had been injected with PBS.

Increased myofibroblast accumulation in the dermis is a key finding in scleroderma and is thought to contribute to pathogenesis. To compare the accumulation of myofibroblasts in the lesional skin of wild-type and MCP-1−/− mice,

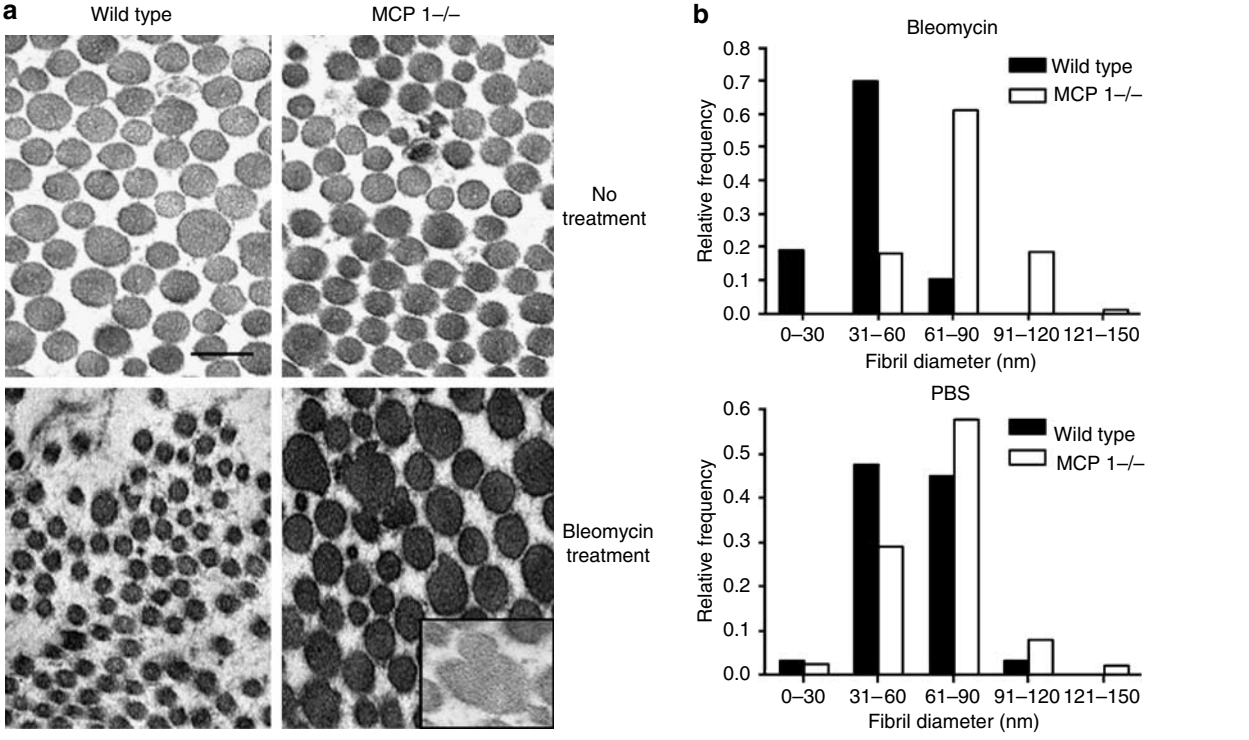

Figure 2. Ultrastructural analysis of collagen fibril content in lesional skin. (**a**) Transmission electronmicroscopy of untreated and bleomycin-treated skin, $n = 4$ for all groups. Transmission electronmicroscopy was performed to examine collagen fibril structure in the dermis of untreated normal skin (upper panels) and bleomycin-treated skin (lower panels) from both WT (left panels) and MCP-1−/− (right panels) mice. Bar = 100 nm. In bleomycin-treated lesional skin from WT mice, the large diameter collagen fibrils normally seen in skin were replaced by smaller fibrils. In contrast, bleomycin-induced lesions from MCP-1−/− mice showed a pattern of fibril diameter and distribution (average diameter, 76.7 ± 6.1 nm) quite similar to untreated normal skin. Inset: higher magnification of large collagen fibrils with irregular shape that were seen in bleomycin-treated skin of MCP-1−/− but not WT mice. These structures may represent fused collagen fibrils. (**b**) Histograms of the distribution of collagen fibril diameter in untreated and bleomycin-treated skin of WT and MCP-1−/− mice. The diameter of individual collagen fibril was determined for between 1,170 and 2,665 fibrils per section. Two separate sections per mouse were examined and four micrographs per mouse representing cross-sections of collagen fibrils were analyzed to generate the histograms. The relative frequency of collagen fibril diameters is shown. The distribution of collagen fibrils in bleomycin-treated skin of WT and MCP-1−/− strains was found to be significantly different ($P = 0.0339$) by Wilcoxon rank-sum test. No significant difference in the distribution of collagen fibrils was found in PBS treatment groups.

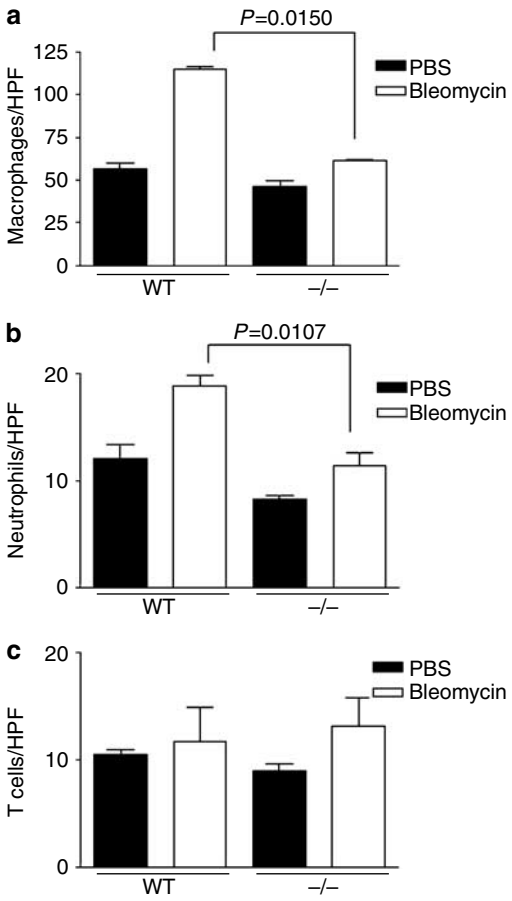

Figure 3. Quantitative immunohistochemical analysis of inflammatory cells in lesions of WT and MCP-1−/− mice. Histologic sections of lesional skin from WT and MCP-1−/− mice were subjected to immunohistochemical staining with (**a**) anti-MOMA (macrophage marker), (**b**) anti-CD3 (T-cell marker), and (**c**) anti-GR-1 (neutrophil marker) antibodies. The number of positive cells was counted in five high-powered fields per section. The results are expressed as means per five high-powered fields (× 200). $n = 3$ for WT and $n = 4$ for MCP-1−/− mice. Statistical analysis was performed using a Student's *t*-test. *P*-values < 0.05 are shown.

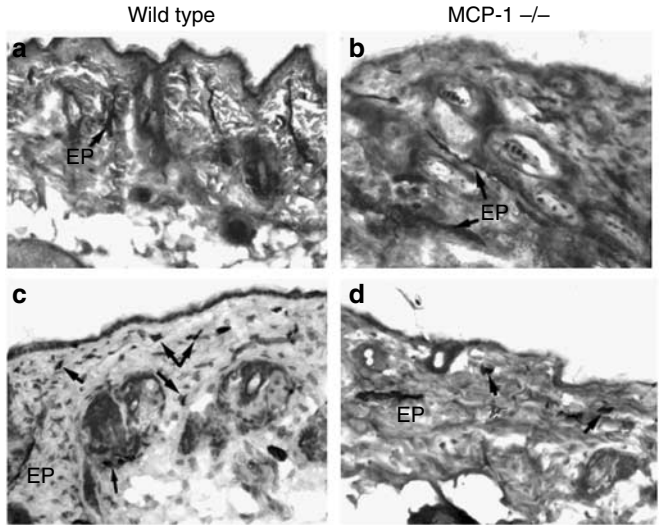

Figure 4. Immunohistochemical detection of myofibroblasts in lesional skin from WT and MCP-1−/− mice. α-SMA staining was performed on tissue sections from (**a** and **b**) PBS or (**c** and **d**) bleomycin treated (**a** and **c**) WT and (**b** and **d**) MCP-1−/− mice. Dark stain indicates positive labeling of myofibroblasts (closed arrow) as well as erector pili muscle (EP). Representative photomicrographs are shown from four animals per group. In WT mice, PBS-treated sites contained few α-SMA-positive cells. In contrast, bleomycin-treated sites of WT mice consistently exhibited α-SMA-positive cells throughout the dermis. In MCP-1−/− mice, few α-SMA-positive cells other than erector pili were seen in either PBS or bleomycin-injected skin. Original magnification × 200. (Color figure available online.)

the expression of alpha-smooth muscle actin (α-SMA) was examined by immunohistochemistry in multiple histologic sections from four mice per group. In normal skin, α-SMA was observed exclusively in vessels and erector pili muscles (data not shown). α-SMA-positive cells other than erector pili were also rare in the area of PBS injection in both wild-type and MCP-1−/− strains (Figure 4a and b). At bleomycin-injection sites, however, myofibroblasts were consistently found to be distributed throughout the dermis of the lesional skin of wild-type mice. By comparison, bleomycin-injected lesional skin from MCP-1−/− mice consistently exhibited only rare myofibroblasts (Figure 4c and d).

Analysis of TGF-β1 and MCP-1 levels

The levels of TGF-β1, as assessed by ELISA, were significantly greater in bleomycin-treated wild-type mice compared to MCP-1−/− mice (0.83 ± 0.23 *vs* 0.47 ± 0.11 pg/μg of total protein). In addition, there were no significant differences between TGF-β1 levels of wild-type and MCP-1−/− mice treated with PBS. Similarly, dermal administration of bleomycin resulted in a significant increase of MCP-1 levels in wild-type mice when compared with mice treated with PBS (64.5 ± 9.9 *vs* 12.59 ± 2.42 pg/μg of total protein).

Differential expression of MMP and TIMPs in bleomycin-treated wild-type and MCP-1−/− mice

As dermal fibrosis may occur as a result of abnormalities in the regulation of collagen synthesis and degradation, we analyzed the expression levels of MMPs and their physiological inhibitors, TIMPs, by RNase protection assay. As shown in Figure 5, when compared to bleomycin-treated skin from wild-type mice, bleomycin-treated skin from MCP-1−/− mice showed a 3-fold increase in the MMP-13, TIMP-2, and TIMP-3 expression levels. There were no remarkable differences in TIMP-1 expression in the lesions of wild-type and MCP-1−/− mice. Further, no MMP-2, MMP-3, MMP-7, MMP-8, MMP-9, and TIMP-4 expression was detected in any group by this RNase protection assay.

Comparison of the gene expression profile of type I collagen, decorin, fibromodulin, and HSP47 between MCP-1−/− and wild-type treated mice

Previous studies have demonstrated that the expression of HSP47, decorin, and fibromodulin are associated with increased deposition of collagen and modulation of collagen

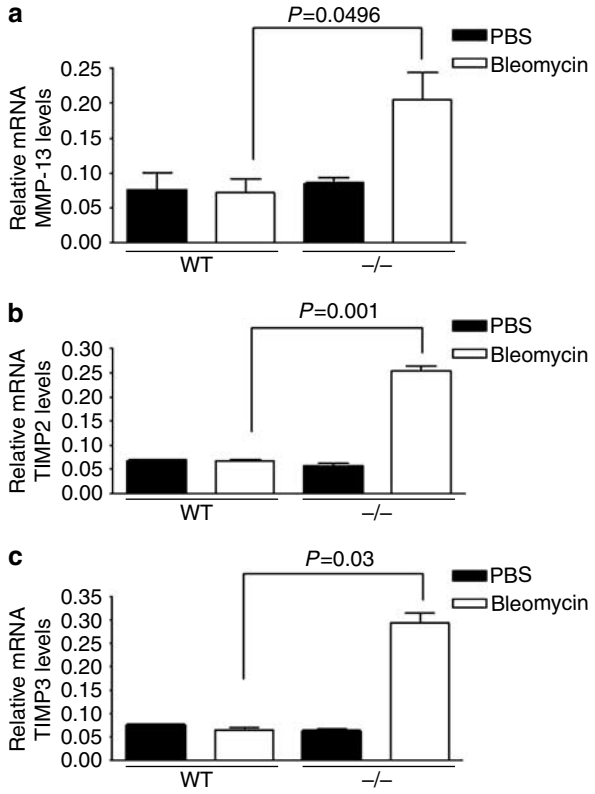

Figure 5. Measurement of MMPs and TIMPs mRNA in lesions of wild type (WT) and MCP-1−/− mice. MCP-1−/− ($n=5$) and WT ($n=4$) mice were injected with bleomycin or PBS for 4 weeks. Total RNA was extracted from lesional skin and the levels of various MMPs and TIMPs were compared by RNase protection assay using RiboQuant MultiProbe. Densitometic analysis of (**a**) MMP13, (**b**) TIMP2, and (**c**) TIMP3 mRNA expression. Specific mRNA levels, detected by RNase protection assay, were normalized to GAPDH expression. Data are representative of two independent experiments where similar results were obtained. Statistical analysis was performed using a Student's *t*-test. *P*-values <0.05 are shown.

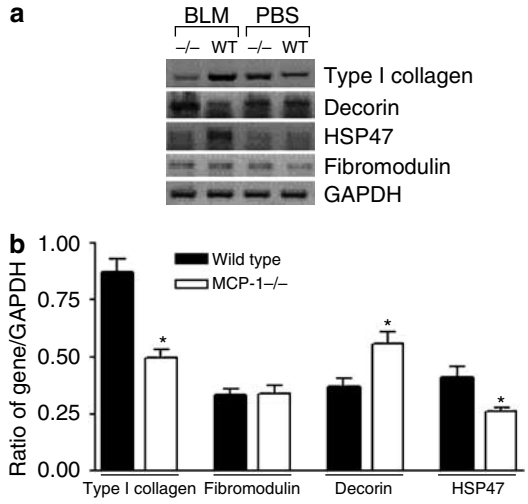

Figure 6. Gene expression profile in skin from MCP-1−/− and WT mice. Total RNA was extracted from the skin from bleomycin- or PBS-treated WT mice ($n=5$) and MCP-1−/− mice ($n=5$). (**a**) Representative gel showing reverse transcriptase-PCR products for murine type I collagen, decorin, fibromodulin, and HSP47. Reverse transcriptase-PCR products were resolved by electrophoresis in a 1.5% agarose gel and analyzed by densitometry. The experiment was repeated two times with identical results. (**b**) Densitometric analysis of gene expression in bleomycin treated skin. The results are depicted graphically as the means ± SE. Statistical analysis was performed using the Student's *t*-test. *$P<0.05$.

fibrillogenesis, contributing to the development of fibrosis (Masuda *et al.*, 1994; Danielson *et al.*, 1997; Iozzo, 1997; Sini *et al.*, 1997; Razzaque *et al.*, 1998; Chakravarti, 2002; Ishii *et al.*, 2003). To determine whether the expression of these key fibrogenic genes was altered in MCP-1−/− mice, semiquantitative reverse transcriptase-PCR was used to determine relative quantities of type I collagen, decorin, fibromodulin, and HSP47 mRNAs in the bleomycin-injection sites. In keeping with the concept that collagen synthesis was reduced in the absence of MCP-1, type I collagen mRNA expression was significantly lower (50%) in the dermis of bleomycin-treated skin of MCP-1−/− mice when compared to wild type (Figure 6a and b). Compared to wild-type lesions, HSP47 mRNA levels were also decreased by approximately 50% in the fibrotic lesions of MCP-1−/− mice. In contrast, levels of decorin mRNA were significantly increased by approximately 52% in MCP-1−/− mice as compared to wild type. No changes in fibromodulin expression were seen between the experimental groups. Taken together, the data suggest that MCP-1 has profound effects on the expression of multiple factors that influence collagen formation and remodeling.

DISCUSSION

MCP-1, a member of the C–C chemokine family, has been characterized as an important chemoattractant for mononuclear cells during inflammation (Rollins, 1996). Recent observations suggest that MCP-1 may be involved in the complex series of events that ultimately result in fibrosis (Yamamoto *et al.*, 2000a; Yamamoto and Nishioka, 2003). More specifically, antibody neutralization of MCP-1 has been shown to decrease bleomycin-induced skin fibrosis (Yamamoto and Nishioka, 2003). Our results support and extend this observation.

MCP-1 is known to be pro-inflammatory, assisting in the recruitment of monocytes and the activation of macrophages (Fuentes *et al.*, 1995). As expected, bleomycin injections elicited a higher accumulation of macrophages in the lesional skin of wild-type mice than in skin from MCP-1−/− mice. These findings are in concert with previous studies of skin injury, as treatment with a neutralizing monoclonal anti-MCP-1 resulted in a decrease in macrophage cell number in dermal wounds (DiPietro *et al.*, 2001). Together, the results support the concept that MCP-1 plays a pivotal role by mediating mononuclear cell recruitment and macrophage activation. The recruited macrophages, via the production of pro-fibrotic cytokines such as TGF-β, may then augment matrix production, fibroblast proliferation, and myofibroblast differentiation (Yamamoto and Nishioka, 2003).

The presence of myofibroblasts is consistent with the pathology of fibrotic diseases (Sappino *et al.*, 1990; Ludwicka *et al.*, 1992). Myofibroblasts are specialized cells with high synthetic capacity for ECM proteins, namely collagen, as well

as fibrogenic cytokines and chemokines (Gabbiani, 2003). Using our model of bleomycin-induced fibrosis, we observed that in addition to increased presence of myofibroblasts, levels of MCP-1 and TGF-β protein were higher in lesional skin of bleomycin-treated wild-type mice. Since MCP-1 is a known inducer of TGF-β and this growth factor was not increased in the skin of bleomycin-treated MCP-1−/− mice, our findings support the concept that MCP-1 sustains the fibrotic process via the direct regulation of TGF-β and also perhaps the consequent myofibroblast accumulation.

Whereas the modulation of inflammation by MCP-1 may be important to the fibrotic response, our studies support the concept of an additional non-inflammatory role for this cytokine. When comparing wild-type and MCP-1−/− mice, the strain-specific differences in matrix organization and collagen fibrillogenesis at the sites of bleomycin injection were striking. In bleomycin-treated MCP-1−/− mice, a modest yet measurable dermal thickening exhibited a collagen arrangement that was near-normal in appearance. In contrast, in wild-type mice (and therefore in the presence of MCP-1) robust dermal thickening was associated with highly disorganized, primary small diameter fibrils, an architecture associated with fibrotic reactions involving rapid ECM accumulation (Kischer, 1974; Fleischmajer *et al.*, 1978; Kahari, 1993; Chen *et al.*, 2003; Lakos *et al.*, 2004). These observations suggest that MCP-1 mediates a sequence of events that ultimately results in the deposition of excess collagen with fibrils that are smaller than in normal skin. The reason for this change in fibrillar size in the lesions of the two strains is not entirely clear. However, our results did reveal that the accumulation of collagen observed in bleomycin-treated skin from wild-type mice is accompanied with an upregulation of HSP47 expression. Since HSP47 plays a crucial role in collagen biosynthesis (Nagai *et al.*, 2000), this change may contribute to the increase synthesis and altered assembly of collagen.

Recent compelling evidence has demonstrated that in scleroderma and other fibrotic diseases, reduced ECM turnover is a contributory factor for collagen accumulation and the development of dermal fibrosis (Nakamura *et al.*, 1993; Milani *et al.*, 1994; Takeda *et al.*, 1994; Arakawa *et al.*, 1996; Ghahary *et al.*, 1996; Hayashi *et al.*, 1996). In the MCP-1−/− mice, enhanced ECM turnover may occur. The turnover of the ECM depends upon the net MMP activity, a characteristic that is derived from the balance between MMPs and TIMPs (Swiderski *et al.*, 1998; Young-Min *et al.*, 2001; Toubi *et al.*, 2002; Sato *et al.*, 2003; Gomez *et al.*, 1997). Our data demonstrates that, as compared to wild-type mice, the balance between MMP and TIMP levels is shifted in the bleomycin-induced lesions of MCP-1−/− mice. In the bleomycin-induced lesions in MCP-1−/− mice, the levels of TIMP-1, which preferentially inhibits the activity of the collagenase MMP-13, remained at basal values, similar to normal skin. MMP-13 levels were increased, a finding in keeping with the concept that enhanced protease activity and thus increased collagen turnover occurs in the lesions of the MCP-1−/− mice. However, the levels of TIMP-2 and TIMP-3 were also significantly upregulated in fibrotic tissue from MCP-1−/− mice. Since TIMP activity would inhibit proteolysis and favor ECM accumulation, these data seems somewhat contradictory to the outcome of increased fibrosis. One possible explanation may be that a substantial increased in the biosynthesis or activity of MMP overcomes the effect of the increased TIMP-2 and TIMP-3 levels, and therefore net MMP levels remain greater in skin lesions from MCP-1−/− mice than in wild-type mice.

One curious observation in the bleomycin lesions of MCP-1−/− mice was the occasional presence of very large fibrils of about 300 nm with abnormal shape. The appearance of these structures is suggestive of aberrant fibril fusion products. Such fusions generally signify a failure to successfully maintain correct interfibrillar spacing. While the reason for such fusion in the MCP-1−/− mice is unknown, the process may involve altered production of particular proteoglycans (Iozzo, 1997). Several members of the small leucine-rich proteoglycans have been shown to interact with fibrillar collagens and thus to influence fibrillar formation. Among them, the appropriate levels of decorin, lumican, and fibromodulin are known to be crucial to the maintenance of correct interfibrillar spacing and to the assembly of the collagen network (Schonherr *et al.*, 1995; Weber *et al.*, 1996). In particular, the addition of exogenous decorin has been shown to cause an increase in the diameter of type I collagen fibrils (Kuc and Scott, 1997). Interestingly, our studies demonstrate increased levels of decorin in MCP-1−/− mice. This increase in decorin production might facilitate collagen fibril fusion. Our results differed from those of Yamamoto *et al.* who showed an increase in decorin expression in fibroblasts in response to MCP-1 treatment (Yamamoto and Nishioka, 2003). This difference may be due to the fact that we examined total decorin expression within fibrotic skin rather than in a primary cell isolate.

The present findings demonstrate a markedly diminished response to fibrotic stimulus in the absence of MCP-1, and are highly supportive of results from other studies in this and other models (Moore *et al.*, 2001; Gharaee-Kermani *et al.*, 2003; Yamamoto and Nishioka, 2003). Several of these previous studies focused on the pro-inflammatory activity of MCP-1, although a direct role for MCP-1 in modulating fibroblast function has been proposed (Yamamoto and Nishioka, 2003). Our results provide new information to indicate that the loss of MCP-1 significantly alters the assembly and accumulation of collagen, adds a new dimension to our understanding of the role of MCP-1 in fibrosis. Importantly, the findings suggest that the role of MCP-1 in fibrosis is multi-factorial, and is not strictly limited to inflammation. Ultimately, inhibition of MCP-1 might be a therapeutic approach to the reduction of scar formation at sites of injury.

MATERIALS AND METHODS

Animals

MCP-1−/− mice, generated as previously described (Gu *et al.*, 1999) were received as homozygous breeder pair from Dr Barrett Rollins. This MCP-1−/− strain, originally derived in C57BL/6-129Sv/J, was backcrossed more than eight generations on a C57BL/6 background

prior to use in this study. This MCP-1−/− strain is viable and fertile, and was maintained in our colony as an inbred strain. As described by others, C57BL/6 mice aged 7–8 weeks, obtained from Jackson Laboratories, were used a control for the MCP-1−/− mice (Lee *et al.*, 2003; Penido *et al.*, 2003; Dewald *et al.*, 2005). Compared to several other strains, the C57BL/6 has been described to exhibit a reduced level of bleomycin-induced skin fibrosis (Yamamoto *et al.*, 2000b). However, the response in this strain is easily measurable, allowing us to use the C57BL/6 as an adequate control for comparison to the MCP-1−/− mice. The animals were maintained on a 12 hours light, 12 hours dark cycle and housed in the animal care facility at Loyola University. All animal procedures followed institutional guidelines. Each study group contained at least four mice.

Bleomycin treatment

Bleomycin (GensiaSicor Pharmaceuticals Inc. Irvine, CA) was diluted to 0.1 U/ml with PBS, sterilized and filtered. Using a 27-gauge needle, 100 μl of bleomycin or PBS was injected subcutaneously into a single location on the shaved back of MCP-1−/− and wild-type mice once daily for 1 or 4 weeks. At the end of the experiments, mice were killed by euthanasia.

Histologic analyses of dermal thickness

Skin samples were obtained from the injected site and embedded in paraffin. Sections (3–5 μm) were cut, mounted on slides, and stained with hematoxylin and eosin or Masson's trichrome. Dermal thickness was measured in hematoxylin and eosin sections viewed under $\times$100 microscopic magnification by measuring the distance between the epidermal–dermal junction and the dermal-fat junction at five randomly selected fields in two or more sections from each animal.

Collagen fibril diameter assessment

Lesional skin from wild-type ($n=4$) or MCP-1−/− mice ($n=4$) was fixed in 4% glutaraldehyde and rinsed in 0.1 M sodium cacodylate buffer. The samples were post-fixed in 1% osmium tetroxide, dehydrated in graded alcohols, and embedded in Spurr's epoxy resin (Electron Microscopy Sciences; Fort, Washington, PA). Ultrathin sections (80 nm) were collected on grids, stained with uracyl acetate and lead citrate and examined with a transmission electron microscope (Hitachi H-600, 75 kv, Pleasonton, CA).

For each mouse, four micrographs representing cross-sections of collagen fibrils were used for quantitative studies. The diameter of between 1,170 and 2,665 individual collagen fibrils per section were measured manually on photographic negatives with a calibrated final original magnification of $\times$30,000 and histograms were generated. The relative frequency for each sample was calculated by dividing the absolute frequency by the total number of data points in the frequency distribution.

Analysis of inflammatory cell infiltrate

Immunohistochemistry was performed on frozen sections as described previously (Swift *et al.*, 1999). Briefly, tissue was embedded in 22-oxacalcitriol (Sakura Finetek, Torrance, CA) and snap frozen. Sections of 10 μm thickness were fixed in acetone for 15 minutes and endogenous peroxidase was blocked with hydrogen peroxide in methanol. Excess proteins were blocked with either 10% normal mouse serum or 10% goat serum for 30 minutes at room temperature. The sections were then incubated for 30 minutes with the primary monoclonal antibodies. For T-cell analysis, monoclonal hamster anti-mouse CD3e (BD-Bioscience, San Jose, CA) was used. For macrophages, rat anti-mouse macrophage antibody (MOMA-2, 1.7 μg/ml, Serotec Inc., Raleigh, NC) was used, and to analyze neutrophils, rat anti-mouse GR-1 (5 μg/ml, RB6-8C5, Pharmingen, San Diego, CA) was used. Following incubation with the primary antibody, sections were washed and incubated for 30 minutes with biotinylated mouse anti-rat IgG (Jackson Immunoresearch, West Grove, PA) at 13 μg/ml for macrophage and neutrophil staining and with biotinylated goat anti-armenian hamster IgG for T cells. Detection was performed using the ABC Elite kit (ABC, Vector Laboratories, Burlingame, CA) followed by incubation in DAB (Kirkegaard and Perry Laboratories, Gaithersburg, MD) for 4 minutes. Finally, the sections were counterstained with hematoxylin (Sigma, St Louis, MO), dehydrated through graded alcohols, and cover slips were applied. For analysis of cell numbers, immunopositive cells were counted in five high-powered fields ($\times$200) per section. The number of positive stained cells was determined for two sections per mouse, and the value expressed as the number of cells per five high-powered fields.

Detection of myofibroblasts in wild-type and MCP-1−/− tissue

Lesional skin from wild-type and MCP-1−/− treated mice was embedded in 22-oxacalcitriol media (Sakura Finetek, Torrance, CA). Sections (10 μm) were cut, mounted on slides, and stained with an antibody for α-SMA (clone 1A4, Sigma, St Louis, MO). Briefly, frozen sections were air dried and fixed with acetone at 4°C for 20 minutes and then rehydrated in PBS for 3 minutes. Subsequently, hydrated sections were quenched with H_2O_2 (0.3%) in 3% normal horse serum for 15 minutes at room temperature. To block endogenous mouse immunoglobulins, the MOM blocking kit (Vector, Burlingame, CA) was used according to the manufacturer's instructions. Slides were then incubated with the supplied biotinylated secondary antibody, reacted with avidin–biotin complex (Vector, Burlingame, CA), and developed with Novared chromogen (Sigma, St Louis, MO), which yields a red color indicating positive staining. Sections were counterstained with hematoxylin, mounted, and analyzed using a Zeiss Axioskop 2 equipped with a Zeiss AxioCam HRc camera (Carl Zeiss, Thornwood, NY). Tissue was collected from four animals per experimental condition, and three sections from each mouse were subjected to immunohistochemical staining for α-SMA-positive cells. A blinded observer examined at least three high-power fields per section. The relative levels of α-SMA-positive cells in lesional, bleomycin-injected sites was described in comparison to levels in control, PBS-injected sites.

Analysis of MMP and TIMP gene expression

Total RNA was isolated from bleomycin- and PBS-treated skin from wild-type and MCP-1−/− mice using Trizol (Invitrogen, Carlsbad, CA), according to the manufacturer's guidelines. Of total RNA, 3 μg was analyzed with the RiboQuant multiprobe RNase protection assay and the mMMP-1 and mMMP-2 mouse metalloproteinase riboprobe template set (BD PharMingen, San Diego, CA) encoding MMP-13, MMP-2, MMP-3, MMP-7, MMP-8, MMP-9, MMP-12, and their inhibitors TIMP-1, TIMP-2, TIMP-3, TIMP-4. Two controls, L32 and glyceraldehyde-3-phosphate-dehydrogenase (GAPDH), were also included in the template set. The hybridization products were

resolved on a polyacrylamide sequencing gel. The gels were dried at 80°C for 1 hour and the mRNA bands were detected with the FX Molecular phosporimaging system. Chemokine mRNA quantification was performed using QuantiOne Molecular Imaging Software (Bio-Rad, Hercules, CA) and the chemokine mRNA bands were normalized to GAPDH bands and the results were expressed as relative OD units ($OD_{gene\ band}/OD_{GAPDH}$).

Analysis of HSP47, type 1 collagen, decorin, and fibromodulin gene expression

Total RNA was extracted from lesional and normal skin biopsy tissue from wild-type ($n=5$) and MCP-1−/− mice ($n=5$) using Trizol (Invitrogen). Of total RNA, 1 μg was reversed transcribed and amplified using the following primers: HSP47 sense 5′-ACCACAG GATGGTGGACAACCGT-3′, antisense 5′-ATCTCGCATCTTGTCTC CCTTGGG-3′; decorin sense 5′-AGTCACAGGGCAGCACCAC-3′, antisense 5′-GGGGATTGTCAGGGTCATAAGG-3′; fibromodulin sense 5′-TGACACAACATGATCTGCAC-3′, antisense 5′-TTCTTGC ACCCCAGTGAGCA-3′; type I collagen sense 5′-TGGTGCCAA GGGTCTCACTGGC-3′, antisense 5′-GGACCTTGTACACCACGT CGTTCACC-3′; GAPDH sense 5′-TGATGACATCAAGAAGGTGGT GAAG-3′, antisense 5′-TCCTTGGAGGCCATGTAGGCCAT-3′. Reverse transcriptase-PCR products were resolved by electrophoresis in a 1.5% agarose gel containing GelStar nucleic acid stain (FMC Bioproducts, Rockland, ME). The bands were visualized and the gels were photographed using a molecular FX Imaging station and Gel Doc (Bio-Rad, Hercules, CA). The optimal number of PCR cycles for each gene was chosen so that all signals for each gene were within the exponential phase.

Protein isolation and ELISA analysis

Lesional and normal skin biopsy tissue from wild-type ($n=3$) and MCP-1−/− mice ($n=3$) was homogenized in protease inhibitor buffer (PBS containing complete protease inhibitor cocktail tablet; Roche Diagnostics, Mannheim, Germany), sonicated, and centrifuged at 10,000 r.p.m. for 10 minutes. Supernatants were used to analyze TGF-β1 and MCP-1 levels by ELISA following the manufacturer's instructions (R&D systems, Minneapolis, MN). TGF-β1 and MCP-1 levels in pg were normalized to total protein concentrations as determined by the Bio-Rad Protein Assay (Bio-Rad, Hercules, CA).

Statistical analysis

All results were evaluated using Graph Pad Prism 4.0 software, and analyzed by a two tailed *t*-test. Data are represented as mean ± SEM. For all analyses, $P<0.05$ was considered significant. For morphometric analysis of collagen fibril diameters, the relative frequency was calculated and the collagen fibril diameter distributions were presented as histograms. Distribution of the means for MCP-1−/− mice was compared with the wild-type group using Wilcoxon Rank-Sum test.

CONFLICT OF INTEREST

The authors state no conflict of interest.

ACKNOWLEDGMENTS

This work was supported by a grant from the National Institutes of Health RO1-GM55238 (L.A.D) and the Dr Ralph and Marian C. Falk Medical Research Trust. We express our thanks to Linda Fox and Mary Kay Olson for the excellent technical assistance and to Dr John McNulty for kindly providing helpful suggestions about quantitative studies of collagen fibril diameters. We thank Dr Barrett J. Rollins for providing the MCP-1−/− strain.

REFERENCES

Arakawa M, Hatamochi A, Mori Y, Mori K, Ueki H, Moriguchi T (1996) Reduced collagenase gene expression in fibroblasts from hypertrophic scar tissue. *Br J Dermatol* 134:863–8

Chakravarti S (2002) Functions of lumican and fibromodulin: lessons from knockout mice. *Glycoconj J* 19:287–93

Chen K, See A, Shumack S (2003) Epidemiology and pathogenesis of scleroderma. *Australas J Dermatol* 44:1–7; quiz 8–9

Dafforn TR, Della M, Miller AD (2001) The molecular interactions of heat shock protein 47 (Hsp47) and their implications for collagen biosynthesis. *J Biol Chem* 276:49310–9

Danielson KG, Baribault H, Holmes DF, Graham H, Kadler KE, Iozzo RV (1997) Targeted disruption of decorin leads to abnormal collagen fibril morphology and skin fragility. *J Cell Biol* 136:729–43

Dewald O, Zymek P, Winkelmann K, Koerting A, Ren G, Abou-Khamis T *et al.* (2005) CCL2/monocyte chemoattractant protein-1 regulates inflammatory responses critical to healing myocardial infarcts. *Circ Res* 96:881–9

DiPietro LA, Reintjes MG, Low QE, Levi B, Gamelli RL (2001) Modulation of macrophage recruitment into wounds by monocyte chemoattractant protein-1. *Wound Repair Regen* 9:28–33

Distler O, Pap T, Kowal-Bielecka O, Meyringer R, Guiducci S, Landthaler M *et al.* (2001) Overexpression of monocyte chemoattractant protein 1 in systemic sclerosis: role of platelet-derived growth factor and effects on monocyte chemotaxis and collagen synthesis. *Arthritis Rheum* 44:2665–78

Fleischmajer R, Gay S, Meigel WN, Perlish JS (1978) Collagen in the cellular and fibrotic stages of scleroderma. *Arthritis Rheum* 21:418–28

Fuentes ME, Durham SK, Swerdel MR, Lewin AC, Barton PS, Megill JR *et al.* (1995) Controlled recruitment of monocytes and macrophages to specific organs through transgenic expression of monocyte chemoattractant protein-1. *J Immunol* 155:5769–76

Gabbiani G (2003) The myofibroblast in wound healing and fibrocontractive diseases. *J Pathol* 200:500–3

Ghahary A, Shen YJ, Nedelec B, Wang R, Scott PG, Tredget EE (1996) Collagenase production is lower in post-burn hypertrophic scar fibroblasts than in normal fibroblasts and is reduced by insulin-like growth factor-1. *J Invest Dermatol* 106:476–81

Gharaee-Kermani M, Denholm EM, Phan SH (1996) Costimulation of fibroblast collagen and transforming growth factor beta1 gene expression by monocyte chemoattractant protein-1 via specific receptors. *J Biol Chem* 271:17779–84

Gharaee-Kermani M, McCullumsmith RE, Charo IF, Kunkel SL, Phan SH (2003) CC-chemokine receptor 2 required for bleomycin-induced pulmonary fibrosis. *Cytokine* 24:266–76

Gomez DE, Alonso DF, Yoshiji H, Thorgeirsson UP (1997) Tissue inhibitors of metalloproteinases: structure, regulation and biological functions. *Eur J Cell Biol* 74:111–22

Gu L, Tseng SC, Rollins BJ (1999) Monocyte chemoattractant protein-1. *Chem Immunol* 72:7–29

Hasegawa M, Sato S, Takehara K (1999) Augmented production of chemokines (monocyte chemotactic protein-1 (MCP-1), macrophage inflammatory protein-1alpha (MIP-1alpha) and MIP-1beta) in patients with systemic sclerosis: MCP-1 and MIP-1alpha may be involved in the development of pulmonary fibrosis. *Clin Exp Immunol* 117:159–65

Hayashi T, Stetler-Stevenson WG, Fleming MV, Fishback N, Koss MN, Liotta LA *et al.* (1996) Immunohistochemical study of metalloproteinases and their tissue inhibitors in the lungs of patients with diffuse alveolar damage and idiopathic pulmonary fibrosis. *Am J Pathol* 149:1241–56

Hunt TK (1990) Basic principles of wound healing. *J Trauma-Injury Infect Crit Care* 30:S122–8

Iozzo RV (1997) The family of the small leucine-rich proteoglycans: key regulators of matrix assembly and cellular growth. *Crit Rev Biochem Mol Biol* 32:141–74

Ishii H, Mukae H, Kakugawa T, Iwashita T, Kaida H, Fujii T *et al.* (2003) Increased expression of collagen-binding heat shock protein 47 in murine bleomycin-induced pneumopathy. *Am J Physiol Lung Cell Mol Physiol* 285:L957–63

Kahari VM (1993) Activation of dermal connective tissue in scleroderma. *Ann Med* 25:511–8

Kischer CW (1974) Collagen and dermal patterns in the hypertrophic scar. *Anat Rec* 179:137–45

Knapp TR, Daniels RJ, Kaplan EN (1977) Pathologic scar formation. Morphologic and biochemical correlates. *Am J Pathol* 86:47–69

Kuc IM, Scott PG (1997) Increased diameters of collagen fibrils precipitated *in vitro* in the presence of decorin from various connective tissues. *Connect Tissue Res* 36:287–96

Lakos G, Takagawa S, Chen SJ, Ferreira AM, Han G, Masuda K *et al.* (2004) Targeted disruption of TGF-beta/Smad3 signaling modulates skin fibrosis in a mouse model of scleroderma. *Am J Pathol* 165:203–17

Lee I, Wang L, Wells AD, Ye Q, Han R, Dorf ME *et al.* (2003) Blocking the monocyte chemoattractant protein-1/CCR2 chemokine pathway induces permanent survival of islet allografts through a programmed death-1 ligand-1-dependent mechanism. *J Immunol* 171:6929–35

Lloyd CM, Minto AW, Dorf ME, Proudfoot A, Wells TN, Salant DJ *et al.* (1997) RANTES and monocyte chemoattractant protein-1 (MCP-1) play an important role in the inflammatory phase of crescentic nephritis, but only MCP-1 is involved in crescent formation and interstitial fibrosis. *J Exp Med* 185:1371–80

Ludwicka A, Trojanowska M, Smith EA, Baumann M, Strange C, Korn JH *et al.* (1992) Growth and characterization of fibroblasts obtained from bronchoalveolar lavage of patients with scleroderma. *J Rheumatol* 19:1716–23

Masuda H, Fukumoto M, Hirayoshi K, Nagata K (1994) Coexpression of the collagen-binding stress protein HSP47 gene and the alpha 1(I) and alpha 1(III) collagen genes in carbon tetrachloride-induced rat liver fibrosis. *J Clin Invest* 94:2481–8

Matrisian LM (1992) The matrix-degrading metalloproteinases. *Bioessays* 14:455–63

Milani S, Herbst H, Schuppan D, Grappone C, Pellegrini G, Pinzani M *et al.* (1994) Differential expression of matrix-metalloproteinase-1 and -2 genes in normal and fibrotic human liver. *Am J Pathol* 144:528–37

Moore BB, Paine R III, Christensen PJ, Moore TA, Sitterding S, Ngan R *et al.* (2001) Protection from pulmonary fibrosis in the absence of CCR2 signaling. *J Immunol* 167:4368–77

Nagai N, Hosokawa M, Itohara S, Adachi E, Matsushita T, Hosokawa N *et al.* (2000) Embryonic lethality of molecular chaperone hsp47 knockout mice is associated with defects in collagen biosynthesis. *J Cell Biol* 150:1499–506

Nakamura T, Ebihara I, Osada S, Takahashi T, Yamamoto M, Tomino Y *et al.* (1993) Gene expression of metalloproteinases and their inhibitor in renal tissue of New Zealand black/white F1 mice. *Clin Sci (London)* 85:295–301

Parks WC (1999) Matrix metalloproteinases in repair. *Wound Repair Regen* 7:423–32

Penido C, Vieira-de-Abreu A, Bozza MT, Castro-Faria-Neto HC, Bozza PT (2003) Role of monocyte chemotactic protein-1/CC chemokine ligand 2 on gamma delta T lymphocyte trafficking during inflammation induced by lipopolysaccharide or *Mycobacterium bovis* bacille Calmette-Guerin. *J Immunol* 171:6788–94

Razzaque MS, Hossain MA, Kohno S, Taguchi T (1998) Bleomycin-induced pulmonary fibrosis in rat is associated with increased expression of collagen-binding heat shock protein (HSP) 47. *Virchows Arch* 432:455–60

Rollins BJ (1996) Monocyte chemoattractant protein 1: a potential regulator of monocyte recruitment in inflammatory disease. *Mol Med Today* 2:198–204

Sappino AP, Schurch W, Gabbiani G (1990) Differentiation repertoire of fibroblastic cells: expression of cytoskeletal proteins as marker of phenotypic modulations. *Lab Invest* 63:144–61

Sato S, Hayakawa I, Hasegawa M, Fujimoto M, Takehara K (2003) Function blocking autoantibodies against matrix metalloproteinase-1 in patients with systemic sclerosis. *J Invest Dermatol* 120:542–7

Schonherr E, Hausser H, Beavan L, Kresse H (1995) Decorin-type I collagen interaction. Presence of separate core protein-binding domains. *J Biol Chem* 270:8877–83

Sini P, Denti A, Tira ME, Balduini C (1997) Role of decorin on *in vitro* fibrillogenesis of type I collagen. *Glycoconj J* 14:871–4

Soo C, Hu FY, Zhang X, Wang Y, Beanes SR, Lorenz HP *et al.* (2000) Differential expression of fibromodulin, a transforming growth factor-beta modulator, in fetal skin development and scarless repair. *Am J Pathol* 157:423–33

Swiderski RE, Dencoff JE, Floerchinger CS, Shapiro SD, Hunninghake GW (1998) Differential expression of extracellular matrix remodeling genes in a murine model of bleomycin-induced pulmonary fibrosis. *Am J Pathol* 152:821–8

Swift ME, Kleinman HK, DiPietro LA (1999) Impaired wound repair and delayed angiogenesis in aged mice. *Lab Invest* 79:1479–87

Takeda K, Hatamochi A, Ueki H, Nakata M, Oishi Y (1994) Decreased collagenase expression in cultured systemic sclerosis fibroblasts. *J Invest Dermatol* 103:359–63

Toubi E, Kessel A, Grushko G, Sabo E, Rozenbaum M, Rosner I (2002) The association of serum matrix metalloproteinases and their tissue inhibitor levels with scleroderma disease severity. *Clin Exp Rheumatol* 20:221–4

Weber IT, Harrison RW, Iozzo RV (1996) Model structure of decorin and implications for collagen fibrillogenesis. *J Biol Chem* 271:31767–70

Yamamoto T, Eckes B, Mauch C, Hartmann K, Krieg T (2000a) Monocyte chemoattractant protein-1 enhances gene expression and synthesis of matrix metalloproteinase-1 in human fibroblasts by an autocrine IL-1 alpha loop. *J Immunol* 164:6174–9

Yamamoto T, Kuroda M, Nishioka K (2000b) Animal model of sclerotic skin. III: Histopathological comparison of bleomycin-induced scleroderma in various mice strains. *Arch Dermatol Res* 292:535–41

Yamamoto T, Nishioka K (2003) Role of monocyte chemoattractant protein-1 and its receptor,CCR-2, in the pathogenesis of bleomycin-induced scleroderma. *J Invest Dermatol* 121:510–6

Yamamoto T, Takagawa S, Katayama I, Yamazaki K, Hamazaki Y, Shinkai H *et al.* (1999) Animal model of sclerotic skin. I: local injections of bleomycin induce sclerotic skin mimicking scleroderma. *J Invest Dermatol* 112:456–62

Young-Min SA, Beeton C, Laughton R, Plumpton T, Bartram S, Murphy G *et al.* (2001) Serum TIMP-1, TIMP-2, and MMP-1 in patients with systemic sclerosis, primary Raynaud's phenomenon, and in normal controls. *Ann Rheum Dis* 60:846–51